# No-scalar hair conjecture in asymptotic de-Sitter spacetime*

Takashi Torii† and Kengo Maeda‡
*Department of Physics, Tokyo Institute of Technology, Meguro-ku, Tokyo 152-0033, Japan*

Makoto Narita§
*Department of Physics, Rikkyo University, Toshima-ku, Tokyo 171-8501, Japan*
(February 7, 2008)

We discuss the no-hair conjecture in the presence of a cosmological constant. For the first step the real scalar field is considered as the matter field and the spacetime is assumed to be static spherically symmetric. If the scalar field is massless or has a convex potential such as a mass term, it is proved that there is no regular black hole solution. For a general positive potential, we search for black hole solutions which support the scalar field with a double well potential, and find them by numerical calculations. The existence of such solutions depends on the values of the vacuum expectation value and the self-coupling constant of the scalar field. When we take the zero horizon radius limit, the solution becomes a boson star like solution which we found before. However new solutions are found to be unstable against the linear perturbation. As a result we can conclude that the no-scalar hair conjecture holds in the case of scalar fields with a convex or double well potential.

04.70.-s, 04.70.Bw, 04.20.Jb, 95.30.Sf



## I. INTRODUCTION

Recent developments of observational techniques have increased interest about black holes and increasing data shows evidence of supermassive black holes in the center of galaxies, and solar mass size black holes which form binary systems. From the theoretical view point, however, there remain many unsolved fundamental issues related to the black holes. One of them is the validity of the black hole no-hair conjecture proposed by Ruffini and Wheeler [1]. The black hole no-hair conjecture states that after the gravitational collapse of the matter field, the resultant black hole approaches stationary spacetime and that all its multipole moments are then uniquely determined by two parameters, $M$ and $a$, which are physically interpreted as the mass and the angular momentum of the black hole. When the source has a net charge $Q$, then of course the parameter is also requested to uniquely determine its (electric and gravitational) multipole moments. The black hole no-hair conjecture is supported by the black hole uniqueness theorems in electrovacuum theories [2] and by the works of Chase [3], Bekenstein [4], Hartle [5] and Teitelboim [6] which show that stationary black hole solutions are hairless in a variety of theories coupling classical fields to Einstein gravity.

However a non-trivial static, spherically symmetric solution, called colored black hole, was discovered in the Einstein-Yang- Mills system [7]. It can be interpreted as the self-gravity of the Yang-Mills field being supported by its repulsive force. Although this solution is found to be unstable both in the gravitational sector [8] and in the sphaleron sector [9], non-Abelian hair is generic and many other non-Abelian black holes were discovered after the colored black hole. Note that some of them are stable and that such solutions are the counterexamples of the black hole no-hair conjecture. The essential difference between the field equations of Einstein-Yang-Mills systems and those of the Einstein-Klein-Goldon system is in the form of the potential term. By using these properties, Bekenstein [4,10] and Sudarsky [11] provided simple proofs for the no-scalar hair theorem in spherically symmetric asymptotically flat spacetime, in the case where the matter consists of a single scalar field with a convex potential and in the extended case where the matter consists of multiple scalar fields with an arbitrary positive potential. Heusler also proved the no-scalar hair theorem by using a scaling technique [12].

Most of the proofs of the no-hair theorems impose, however, asymptotic flatness. Hence the following natural question arises: *Can we extend no-hair theorems to spacetimes with different asymptotic structure?* This is the main

*TIT/HEP-403
†electronic mail:torii@th.phys.titech.ac.jp
‡electronic mail:maeda@th.phys.titech.ac.jp
§electronic mail:narita@se.rikkyo.ac.jp

issue of this paper. Here we consider the system including the cosmological constant and only one real scalar field as a matter field for the first step. The importance of the cosmological constant comes not only from the theoretical aspect but also from the observational results of our universe. For example some astrophysicists have pointed out that the small cosmological constant may explain the observed number count of galaxies [13], and the recent observation of the type Ia supernova at large redshift also supports the universe with a cosmological constant [14]. Furthermore, in the early universe, we usually expect a vacuum energy, which is equivalent to the cosmological constant. As for the black hole solutions with a cosmological constant, the family of the Kerr-Newman-de Sitter solutions are known as the exact solutions. Besides these the cosmic colored black hole solution is derived [15]. These solutions are an extension of the Kerr-Newman solutions and the colored black hole to the non-zero cosmological constant case. Interestingly, although there are black hole solutions in the Einstein- Maxwell-dilaton system [16], no black hole solution exists if we take the cosmological constant into account [17]. Hence the cosmological constant can strongly affect the existence of black hole solutions.

If we find the physical solutions with scalar hair, the no-scalar hair conjecture can not hold in asymptotic de Sitter spacetime and such solutions may have an influence on the cosmology. If there are no such solutions, we can say that the no-scalar hair conjecture holds in our system. In other words, the weak cosmic no-hair conjecture holds in the sense that all initially expanding universes with positive cosmological constant approach the "de Sitter spacetime" asymptotically, except for locally distributed black holes. [18]. Hence it must be stressed that the black hole no-hair conjecture in asymptotic de Sitter spacetime is strongly related to the weak cosmic no-hair conjecture.

This paper is organized as follows. In section II we introduce the model and the basic equations and try to extend the no-hair theorem in a spherically symmetric system. In section III we derive black hole solutions numerically in the model that the real scalar field has a double well potential and discuss their properties. We investigate the stability of these solutions in section IV. We give our conclusions and remarks in the final section.

## II. MODEL AND BASIC EQUATIONS

We will consider the model given by the action

$$S=\int d^4x\sqrt{-g}\left[\frac{1}{16\pi G}(R-2\Lambda)-\frac{1}{2}(\nabla\phi)^2-V(\phi)\right], \tag{1}$$

where $\phi$ is the real scalar field and $V(\phi)$ is its potential. We shall assume a spherically symmetric spacetime and adopt the Schwarzschild type metric,

$$ds^2=-\left(1-\frac{2Gm}{r}-\frac{\Lambda}{3}r^2\right)e^{-2\delta}dt^2+\left(1-\frac{2Gm}{r}-\frac{\Lambda}{3}r^2\right)^{-1}dr^2+r^2\left(d\theta^2+\sin^2\theta d\varphi^2\right). \tag{2}$$

The mass function $m$ and the lapse function $\delta$ depend on both the time coordinate $t$ and the radial coordinate $r$. The mass function is the quasilocal mass defined by Ref. [19], which is the gravitational energy subtracted by the energy due to the cosmological constant $\Lambda$. In other words, it is considered as the energy of the matter field. In spherically symmetric spacetime, the energy $m$ is nondecreasing in the outgoing null or spacelike direction in the region $1-2Gm/r-3\Lambda r^2>0$ if the matter fields satisfy the dominant energy condition.

Varying the action (1) and substituting *Ansatz* (2), we derive the field equations

$$\tilde{m}'=4\pi\tilde{r}^2\left\{\frac{1}{2}\left(1-\frac{2\tilde{m}}{\tilde{r}}-\frac{1}{3}\tilde{r}^2\right)^{-1}e^{2\delta}\dot{\tilde{\phi}}^2+\frac{1}{2}\left(1-\frac{2\tilde{m}}{\tilde{r}}-\frac{1}{3}\tilde{r}^2\right)\tilde{\phi}'^2+\tilde{V}(\tilde{\phi})\right\}, \tag{3}$$

$$\delta'=-4\pi\tilde{r}\left[\left(1-\frac{2\tilde{m}}{\tilde{r}}-\frac{1}{3}\tilde{r}^2\right)^{-2}e^{2\delta}\dot{\tilde{\phi}}^2+\tilde{\phi}'^2\right], \tag{4}$$

$$\dot{\tilde{m}}=4\pi\tilde{r}^2\left(1-\frac{2\tilde{m}}{\tilde{r}}-\frac{1}{3}\tilde{r}^2\right)\dot{\tilde{\phi}}\tilde{\phi}', \tag{5}$$

$$-\left[e^{\delta}\left(1-\frac{2\tilde{m}}{\tilde{r}}-\frac{1}{3}\tilde{r}^2\right)^{-1}\dot{\tilde{\phi}}\right]^{\cdot}+\frac{1}{\tilde{r}^2}\left[\tilde{r}^2e^{-\delta}\left(1-\frac{2\tilde{m}}{\tilde{r}}-\frac{1}{3}\tilde{r}^2\right)\tilde{\phi}'\right]'=e^{-\delta}\frac{d\tilde{V}(\tilde{\phi})}{d\tilde{\phi}}. \tag{6}$$

Here, we have used the dimensionless variables, $\tilde{t} \equiv \sqrt{\Lambda}t$, $\tilde{r} \equiv \sqrt{\Lambda}r$, $\tilde{m} \equiv \sqrt{\Lambda}Gm$, $\tilde{\phi} \equiv \sqrt{G}\phi$ and $\tilde{V} \equiv GV/\Lambda$. A dot and a prime in the field equations denote derivatives with respect to $\tilde{t}$ and $\tilde{r}$, respectively. In this section and the next section we consider only the static solutions, hence we drop the time derivative term of the field equations for a while.

For the boundary conditions of the metric functions on the black hole event horizon (BEH) and on the cosmological event horizon (CEH), we impose the following three *Ansätze*.

(i) The existence of a regular BEH $r_B$; i.e.,

$$2Gm(r_B) = r_B\left(1 - \frac{\Lambda}{3}r_B^2\right), \tag{7}$$

$$\delta(r_B) < \infty. \tag{8}$$

(ii) The existence of a regular CEH $r_C$; i.e.,

$$2Gm(r_C) \equiv 2GM = r_C\left(1 - \frac{\Lambda}{3}r_C^2\right), \tag{9}$$

$$\delta(r_C) < \infty. \tag{10}$$

Here we assume $\delta(r_C) = 0$. Note that if we are interested in a different boundary condition such as $\delta \to \delta^* \neq 0$, we can always have such a boundary condition without further calculation by rescaling the time coordinate. That is, introducing $\bar{\delta} \equiv \delta - \delta^*$, and rescaling the time coordinate as $\bar{t} = e^{-\delta^*}\tilde{t}$, we recover our boundary condition.

(iii) The non-existence of singularity between BEH and CEH; i.e., for $r_B < r < r_C$,

$$2Gm(r) < r\left(1 - \frac{\Lambda}{3}r^2\right). \tag{11}$$

As for the scalar field, we impose the finiteness of itself and its derivatives. These conditions guarantee that the curvature invariant $I = R_{\mu\nu\rho\sigma}R^{\mu\nu\rho\sigma}$ is finite and that no naked singularity appears.

Now we investigate whether or not the no-scalar hair theorems obtained by Bekenstein [4,10] and Sudarsky [11] can be extended to our system. First we consider the case of the scalar field with convex potential, e.g. $V(\phi) = m_\phi^2\phi^2$. In the static spacetime the equation of the scalar field is

$$\left(\tilde{r}^2 e^{-\delta} f\tilde{\phi}'\right)' = \tilde{r}^2 e^{-\delta}\frac{d\tilde{V}(\tilde{\phi})}{d\tilde{\phi}}, \tag{12}$$

where $f = 1 - 2\tilde{m}/\tilde{r} - \tilde{r}^2/3$. Multiplying by $\tilde{\phi}$ and integrating from BEH to CEH, we obtain

$$\begin{aligned}
&\int_{\tilde{r}_B}^{\tilde{r}_C} d\tilde{r}\left\{\tilde{r}^2 e^{-\delta}\tilde{\phi}\frac{d\tilde{V}(\tilde{\phi})}{d\tilde{\phi}} - \tilde{\phi}\left(\tilde{r}^2 e^{-\delta} f\tilde{\phi}'\right)'\right\} \\
&\quad = \int_{\tilde{r}_B}^{\tilde{r}_C} d\tilde{r}\tilde{r}^2 e^{-\delta}\left(\tilde{\phi}\frac{d\tilde{V}(\tilde{\phi})}{d\tilde{\phi}} + f\tilde{\phi}'^2\right) - \left[\tilde{r}^2 e^{-\delta} f\tilde{\phi}\tilde{\phi}'\right]_{\tilde{r}_B}^{\tilde{r}_C} \\
&\quad = \int_{\tilde{r}_B}^{\tilde{r}_C} d\tilde{r}\tilde{r}^2 e^{-\delta}\left(\tilde{\phi}\frac{d\tilde{V}(\tilde{\phi})}{d\tilde{\phi}} + f\tilde{\phi}'^2\right) = 0
\end{aligned} \tag{13}$$

Since $\tilde{V}$ is a convex potential, the integrand is positive semi-definite. Hence the possible solution is $\tilde{\phi} \equiv 0$. As a result the same argument as Bekenstein's holds and the no-scalar hair theorem is complete in the convex potential case [20]. When the scalar field is massless, i.e., $\tilde{V} \equiv 0$, Eq. (13) also demands $\tilde{\phi} \equiv 0$, which is the no-hair theorem for a massless scalar field.

Next we proceed to the theorem proved by Sudarsky. First we rewrite Eq. (6) in the static spacetime as

$$\left(e^{-\delta} f\tilde{\phi}'\right)' + \frac{2}{\tilde{r}}e^{-\delta} f\tilde{\phi}' - e^{-\delta}\frac{d\tilde{V}(\tilde{\phi})}{d\tilde{\phi}} = 0. \tag{14}$$

Multiplying $\tilde{\phi}'$ and integrating once, we obtain

$$E' = -ae^{-\delta}\tilde{\phi}'^2, \tag{15}$$

where

$$E = e^{-\delta}\left(f\tilde{\phi}'^2 - \tilde{V}\right), \tag{16}$$

$$a = \frac{2}{\tilde{r}}\left(1 - \frac{3\tilde{m}}{2\tilde{r}} - \frac{1}{2}\tilde{r}^2\right). \tag{17}$$

In the $\Lambda = 0$ case, i.e., asymptotically flat case, $E = -\tilde{V} < 0$ on BEH, and $a$ is always positive between BEH and CEH because of the regularity. (Note that we have normalized variables by $\Lambda$, $a = 2(1 - 3m/2r)/r$ in the $\Lambda = 0$ case.) Hence $E$ decreases monotonically and then becomes negative everywhere. However $E$ must approach zero in the asymptotic region [11]. This means that there is no regular solution in this system. On the other hand, in the $\Lambda \neq 0$ case, $E = -\tilde{V} < 0$ on both horizons and $a$ is no longer positive definite. Hence the inconsistent behavior of $E$ can not be derived from Eq. (15). Furthermore asymptotic behavior does not reject the scalar hair in the arbitrarily positive potential case [20].

This suggests that the method adopted here may not be appropriate to prove the black hole no-hair or that the black hole solutions with non-trivial scalar hairs may exist. We will search for such solutions in the next section by using numerical calculations.

## III. BLACK HOLE SOLUTIONS WITH SCALAR HAIR

In this section we investigate the system including a double well potential $V(\phi) = \lambda(\phi^2 - v^2)^2/4$ as an example of a positive potential. In this case there are two trivial black hole solutions. One is (a) $\tilde{\phi} \equiv \tilde{v}$, $\tilde{m} \equiv \tilde{M}$, $\delta \equiv 0$. The scalar field takes its vacuum expectation value and does not contribute to the spacetime at all. This is the usual Schwarzschild-de Sitter solution. The other is (b) $\tilde{\phi} \equiv 0$, $\tilde{m} = \tilde{M} + \pi\tilde{\lambda}\tilde{v}^2\tilde{r}^3/3$, $\delta \equiv 0$, where $\tilde{\lambda} \equiv \lambda/G\Lambda$ and $\tilde{v} \equiv \sqrt{G}v$. The scalar field sits on the top of the potential barrier everywhere and its contribution to the spacetime can be interpreted as the "effective cosmological constant" defined by $\Lambda_{eff} = 2\pi\lambda\tilde{v}^4$. We call this solution the excited Schwarzschild-de Sitter solution.

The equation of the scalar field (6) is rewritten as

$$f\tilde{\phi}'' + \left[\left(\frac{2}{\tilde{r}} + 4\pi\tilde{r}\tilde{\phi}'^2\right)f + f'\right]\tilde{\phi}' = \tilde{\lambda}\tilde{\phi}\left(\tilde{\phi}^2 - \tilde{v}^2\right). \tag{18}$$

On the event horizon Eq. (18) becomes

$$f'\tilde{\phi}' = \tilde{\lambda}\tilde{\phi}\left(\tilde{\phi}^2 - \tilde{v}^2\right). \tag{19}$$

Since $f'$ is positive on the BEH, $\phi'(r_B) > 0$ if $-v < \phi(r_B) < 0$, $v < \phi(r_B)$, and $\phi'(r_B) < 0$ if $\phi(r_B) < -v$, $0 < \phi(r_B) < v$. On the other hand $f'$ is negative on the CEH, $\phi'(r_C) > 0$ if $\phi(r_C) < -v$, $0 < \phi(r_C) < v$ and $\phi'(r_C) < 0$ if $-v < \phi(r_C) < 0$, $v < \phi(r_C)$. At the extremum point of $\phi$, Eq. (18) becomes

$$f\tilde{\phi}'' = \tilde{\lambda}\tilde{\phi}\left(\tilde{\phi}^2 - \tilde{v}^2\right). \tag{20}$$

Since $f$ is always positive between BEH and CEH, $\phi$ has no local maximum if $-v < \phi(r) < 0$, $v < \phi(r)$ and $\phi$ has no local minimum if $\phi(r) < -v$, $0 < \phi(r) < v$. Now we estimate the possible behavior of the scalar field from the above constraints. We can restrict $\phi(r_B) > 0$ without loss of generality because the scalar field has reflection symmetry. If $\phi(r_B) > v$, $\phi$ increases around the BEH. Since there is no maximum point $\phi > v$, it continues to increases monotonically to the CEH. However on the CEH $\phi'$ must be negative. This is a contradiction. When $0 < \phi(r_B) < v$, $\phi$ decreases around the BEH. Since there is no minimum in this region, $\phi$ must pass over the potential barrier ($\phi = 0$). Continuing to decrease beyond $\phi = -v$, $\phi$ can not satisfy the boundary condition on the CEH because $\phi$ has no minimum in $\phi < -v$. Hence $\phi$ must stop at a certain value in $-v < \phi < 0$ or have a minimum. In the latter case $\phi$ passes over the potential barrier again. In this way $\phi$ may oscillate any number of times and takes a value $-v < \phi < v$ on the CEH. For each oscillation $\phi$ has to go over the potential barrier.

Now we search for non-trivial static solutions using numerical analysis. We drop the time derivative term of the field equations (3), (4) and (6) and integrate them from the BEH with the boundary conditions (7) and (8). Since the equation of the scalar field (6) becomes singular on the event horizons, we expand the equation and variables by power series of $\tilde{r} - \tilde{r}_B$ to guarantee the regularity on the BEH, and use their analytic solutions for the first step of

integration. For most of the values of $\tilde{\phi}(\tilde{r}_B)$, the scalar field diverges as the integration approaches the CEH. Hence we have to find a suitable value of $\tilde{\phi}(\tilde{r}_B)$ in order to satisfy the boundary conditions (9) and (10). In this sense $\tilde{\phi}(\tilde{r}_B)$ is a shooting parameter.

We found the non-trivial solutions when $\tilde{\lambda}$, $\tilde{v}$ and $\tilde{r}_B$ satisfy a certain condition which will discussed later. They are classified into several families by the node number $n$ of the scalar field. Configurations of the field functions of the solutions with $\tilde{\lambda} = 700$, $\tilde{v} = 0.1$ and $n = 1$ for different radii of BEH are shown in Fig. 1. The left and right end points of each solid line are BEH and CEH, respectively. A dotted line traces them. A dashed line is the regular solution, which can be considered as the solutions in $\tilde{r}_B \to 0$ limit [21]. The structures of the new solutions do not concentrate around the BEH but spread out to a cosmological scale. As the BEH becomes large, the CEH becomes small and the values of the scalar field on each event horizon approaches its vacuum value $\tilde{\phi} = \pm\tilde{v}$. Hence the scalar field must vary rapidly in a small region and become steep. However, as the BEH becomes even larger, $\tilde{\phi}(\tilde{r}_B)$ and $\tilde{\phi}(\tilde{r}_C)$ approach zero and finally BEH and CEH coincide to be the extremal solution.

We show the $\tilde{\lambda}$ dependence of the scalar field for $\tilde{r}_B = 0.2$, $\tilde{v} = 0.1$ and $n = 1$ in Fig. 2. For large $\tilde{\lambda}$, which can be considered as the case that the cosmological constant is small, the scalar field remains at its vacuum value $\tilde{\phi} \approx \tilde{v}$ even for quite large $\tilde{r}$ around the BEH. As $\tilde{\lambda}$ decreases, the amplitude of $\tilde{\phi}$ becomes small and finally the solution coincides with the excited Schwarzschild-de Sitter solution (b) at a certain critical value $\tilde{\lambda}_{min} \cong 354.8$. These properties are qualitatively the same as the regular solution discussed in Ref. [21]. For different values of parameters $\tilde{v}$, we obtain similar results to those mentioned above.

We show the $\tilde{M} - \tilde{r}_B$ diagram of new solutions in Fig. 3, where $\tilde{M}$ is the quasi-local mass on the CEH. We fix $\tilde{v} = 0.1$ and $n = 1$. We also show (a) the Schwarzschild-de Sitter branch and (b) the exited Schwarzschild-de Sitter branch by dashed and dotted lines, respectively, for comparison. We find that each solution branch turns at $\tilde{M} = 1/3$. From the boundary condition (9)

$$M = \frac{r_C}{2G}\left(1 - \frac{\Lambda}{3}{r_C}^2\right). \tag{21}$$

Since the BEH has a one to one correspondence to the CEH around the turning point,

$$\frac{\partial M}{\partial r_B} = \frac{\partial r_C}{\partial r_B}\frac{\partial M}{\partial r_C} = \frac{1}{2}\frac{\partial r_C}{\partial r_B}\left(1 - \Lambda r_C^2\right) = 0, \tag{22}$$

on the turning point. From Fig. 3, $\partial r_C/\partial r_B$ does not vanish, hence $\tilde{r}_C = \sqrt{\Lambda} r_C = 1$ at the turning point. This means $\tilde{M} = 1/3$.

The properties of the new solution branch are quite different depending on $\tilde{\lambda}$. For small $\tilde{\lambda}$ there is only one solution for each BEH radius. As the BEH radius increases, the branch approaches the excited Schwarzschild-de Sitter branch and finally both branches coincide at the maximum BEH radius. At this point the BEH and CEH coincide and the solution becomes extremal. There is the minimum BEH radius, below which only trivial solutions, i.e., Schwarzschild-de Sitter solutions (a) and (b) exist. The non-trivial branch is very close to the excited Schwarzschild-de Sitter branch. As we can see in Fig. 2, the scalar field remains near the top of the potential barrier ($\phi \sim 0$) for small $\tilde{\lambda}$. The main contribution to $M$ must be this potential energy of the scalar field. Hence the solution is similar to the excited Schwarzschild-de Sitter solution.

On the other hand, for large $\tilde{\lambda}$, there are two solutions, which have the same BEH radius. This only occurs for a narrow range of radii The maximum BEH radius is not at the extremal point but a turning point plotted by dots in Fig. 3. On the small BEH radius , we can take the $r_B \to 0$ limit even for the non-trivial branch, and the solution becomes the regular solution [21]. From Fig. 2 the scalar field takes an almost vacuum value near both horizons and passes rapidly on the top of the potential barrier. As a result the non-trivial branch is quite different from the excited Schwarzschild-de Sitter solution.

In Fig. 4 we show the critical parameters in the $\tilde{\lambda} - \tilde{v}$ plane for $r_B = 0.6$ and $n = 1$. There is a solution only in the region between $\tilde{\lambda}_{mim}$ and $\tilde{\lambda}_{max}$. The existence of the critical line $\tilde{\lambda}_{min}$ plotted by the dashed line is due to reasons similar to those in the regular solution case. In the regular solution case the critical lines are derived by investigating the perturbation from the de Sitter solution and are expressed as $(\tilde{R}_{cos}/\tilde{\lambda}_{Comp})^2 = n(2n+3)$, where $\tilde{R}_{cos} = \sqrt{3/(1 + 2\pi\tilde{\lambda}\tilde{v}^4)}$ is the typical scale of the CEH, $\tilde{\lambda}_{Comp} = \sqrt{2/\tilde{\lambda}\tilde{v}^2}$ is the typical size of the structure and $n$ is the node number of the scalar field [21]. If $\tilde{\lambda}$ becomes small, the size of the structure becomes large compared to the size of the CEH. Below the critical parameter $\tilde{\lambda}_{cr}$ the structure can not be packed into the radius $\tilde{R}_{cos}$ and the non-trivial solution disappears. Let us consider the effect of the existence of the BEH to the critical parameter. Rescaling $\tilde{r}$ and $\tilde{m}$ by the BEH radius $\tilde{r}_B$ as $\bar{r} \equiv \tilde{r}/\tilde{r}_B$ and $\bar{m} \equiv \tilde{m}/\tilde{m}_B$, and taking an approximation $\tilde{\phi} \gg \tilde{\phi}' \approx 0$, i.e., near the critical parameter $\tilde{\lambda}_{min}$, the field equations become

$$\frac{d\bar{m}}{d\bar{r}} \approx \tilde{\lambda}\tilde{r}_B^2\bar{r}^2(\tilde{\phi}^2-\tilde{v}^2)^2, \tag{23}$$

$$\frac{d\bar{\delta}}{d\bar{r}} \approx 0, \tag{24}$$

$$\tilde{\lambda}\tilde{r}_B^2\tilde{\phi}(\tilde{\phi}^2-\tilde{v}^2) \approx 0, \tag{25}$$

where $\tilde{\lambda}\tilde{r}_B^2$ can be considered as the effective self-coupling constant and the critical solutions are controlled by it. Consequently $\tilde{\lambda}_{min}$ becomes small when we consider the large BEH radius.

On the other hand $\tilde{\lambda}_{max}$ is a new restriction which can not be seen in the regular solution case. From Fig. 3 the maximum BEH radius for each $\tilde{\lambda}$ branch becomes small as $\tilde{\lambda}$ increases. Hence if we fix the BEH radius, the non-trivial solution disappears at a certain critical value of $\tilde{\lambda}$. This is a $\tilde{\lambda}_{max}$ curve. The types of the critical solutions are different depending on $\tilde{\lambda}_{max}$ or equivalently $\tilde{v}_{max} \equiv \tilde{v}(\tilde{\lambda}=\tilde{\lambda}_{max})$. When $\tilde{v}_{max} \gtrsim 0.14$ for $\tilde{r}_B = 0.6$ the critical solution is the extremal solution. Otherwise the critical solution is not the extremal one, but is shown by the points plotted on the solution for $\tilde{\lambda} = 2000$, 5000 in Fig. 3.

## IV. STABILITY ANALYSIS

In the previous section we found black hole solutions with scalar hair in de Sitter spacetime although there is no counterpart in asymptotically flat spacetime. This means that the no-hair conjecture may not hold in asymptotic de Sitter spacetime. In this section we investigate the stability of new solutions by using a linear perturbation method in order to check whether the scalar hair is really physical or not. Here we focus only on the radial modes.

First we expand the field functions around the static solution $\tilde{\phi}_0$, $\tilde{m}_0$ and $\delta_0$ as follows:

$$\tilde{\phi}(\tilde{t},\tilde{r}) = \tilde{\phi}_0(\tilde{t}) + \frac{\tilde{\phi}_1(\tilde{t},\tilde{r})}{\tilde{r}}\epsilon, \tag{26}$$

$$\tilde{m}(\tilde{t},\tilde{r}) = \tilde{m}_0(\tilde{t}) + \tilde{m}_1(\tilde{t},\tilde{r})\epsilon, \tag{27}$$

$$\delta(\tilde{t},\tilde{r}) = \delta_0(\tilde{t}) + \delta_1(\tilde{t},\tilde{r})\epsilon. \tag{28}$$

Here $\epsilon$ is an infinitesimal parameter. Substituting them into the field functions (3) $\sim$ (6) and dropping the second and higher order terms of $\epsilon$, we find

$$\dot{\tilde{m}}_1 = 4\pi\tilde{r}^2 f_0\tilde{\phi}_0'\dot{\tilde{\phi}}_1, \tag{29}$$

$$-e^{\delta_0}f_0^{-1}\ddot{\tilde{\phi}}_1 + \left[e^{-\delta_0}f_0\tilde{\phi}_1'\right]' - \left[\frac{1}{\tilde{r}}\left(e^{-\delta_0}f_0\right)' + 8\pi\tilde{r}e^{-\delta_0}\lambda(\tilde{\phi}_0^2-\tilde{v}^2)\tilde{\phi}_0\tilde{\phi}_0' + \lambda e^{-\delta_0}(3\tilde{\phi}_0^2-\tilde{v}^2)\right]\tilde{\phi}_1$$
$$-\left[\frac{2}{\tilde{r}}\left(\tilde{r}e^{-\delta_0}\tilde{\phi}_0'\right)' - 8\pi\tilde{r}e^{-\delta_0}\tilde{\phi}_0'^3\right]\tilde{m}_1 = 0, \tag{30}$$

where $f_0 = 1-2\tilde{m}_0/\tilde{r}-1/3$. Next we set $\tilde{\phi}_1 = \xi(\tilde{r})e^{i\tilde{\sigma}\tilde{t}}$ and $\tilde{m}_1 = \eta(\tilde{r})e^{i\tilde{\sigma}\tilde{t}}$. If $\tilde{\sigma}$ is real, $\phi$ oscillates around the static solution and then the solution is stable. On the other hand, if the imaginary part of $\tilde{\sigma}$ is negative, the perturbation $\tilde{\phi}_1$ and $\tilde{m}_1$ diverges exponentially with time and then the solution is unstable. By Eq. (29) the relation between $\xi$ and $\eta$ is $\eta = 4\pi\tilde{r}f_0\tilde{\phi}_0'\xi$. Then the perturbation equation of the scalar field becomes

$$-\frac{d^2\xi}{d\tilde{r}^{*2}} + \tilde{U}(\tilde{r})\xi = \tilde{\sigma}^2\xi, \tag{31}$$

where we employ the tortoise coordinate $\tilde{r}^*$ defined by

$$\frac{d\tilde{r}^*}{d\tilde{r}} = \frac{e^{\delta_0}}{f_0}, \tag{32}$$

and the potential function is

$$\tilde{U}(r) = e^{-\delta_0}f_0\left[\frac{1}{\tilde{r}}\left(e^{-\delta_0}f_0\right)' + 8\pi\tilde{r}e^{-\delta_0}\lambda(\tilde{\phi}_0^2-\tilde{v}^2)\tilde{\phi}_0\tilde{\phi}_0' + \lambda e^{-\delta_0}(3\tilde{\phi}_0^2-\tilde{v}^2)\right.$$
$$\left.+4\pi\tilde{r}f_0\tilde{\phi}_0'\left\{\frac{2}{\tilde{r}}\left(\tilde{r}e^{-\delta_0}\tilde{\phi}_0'\right)' - 8\pi\tilde{r}e^{-\delta_0}\tilde{\phi}_0'^3\right\}\right]. \tag{33}$$

Fig. 5(a) shows the potential functions $U(r)$ of the solution with $\tilde{\lambda} = 300$, $\tilde{v} = 0.1$ and $n = 1$.

Since $d^2\xi/d\tilde{r}^{*2} = U(r) = 0$ on both horizons, $\xi$ must approach zero as $\tilde{r}^* \to \pm\infty$ for the negative mode by the regularity of Eq. (31). Under this boundary condition we have searched for the negative eigenmodes and found them as shown in Fig. 5(b). These modes are bound states ($m = 0$) and there is no excited mode ($m = 1$) for $n = 1$. For the solution with $n = 2$, however, there are two negative modes. We expect that the node number of the scalar field of the static solution $n$ exactly corresponds to the number of their negative modes $m$. Fig. 5(c) gives the eigenvalues. We also plot the eigenvalues of the excited Schwarzschild-de Sitter case with dashed lines for comparison. At the point $P$, where the new solution branch coincides with the Schwarzschild-de Sitter branch, another unstable mode, which is an excited mode, appears in the Schwarzschild-de Sitter branch. This result is consistent with the analysis using catastrophe theory [22,23], and this stability change is classified into the swallow tail catastrophe. Although there is the $r_B \to 0$ limit for large $\tilde{\lambda}$ as we mentioned, the eigenvalue does not vary continuously to that of the regular solution because of the difference of the boundary condition around the origin. Varying the parameters we found negative eigenmodes for every non-trivial solution. As a result, all of the new solutions are unstable, even against the radial perturbations and the scalar hair falls out easily. Thus, although we found black hole solutions with scalar hair in the presence of cosmological constant, such hair is not physical and the no-hair conjecture seems to hold even in the de Sitter spacetime.

## V. CONCLUSION

We examined the no-hair conjecture in the presence of a cosmological constant. For the first step, the real scalar field was considered as the matter field and the spacetime was assumed to be static spherically symmetric. When the scalar field is massless or has a convex potential like mass term, it was proved that there is no regular black hole solution. However we can not find any proof excluding scalar hair in the general positive potential case. Therefore we searched for black hole solutions which have a scalar field with a double well potential, and found them by numerical calculations. Their field configurations spread out to the cosmological scale and are classified by the node number of the scalar field. For large BEH a solution branch ends up with the extreme solution in the $\tilde{M}$-$\tilde{r}_B$ diagram, while for small BEH the behavior is different, depending on the self- coupling constant $\tilde{\lambda}$. If $\tilde{\lambda}$ is large, we can take the limit $\tilde{r}_B \to 0$ and the corresponding solution becomes regular a solution without the BEH. If $\tilde{\lambda}$ is small, the new solution branch hits the excited Schwarzschild-de Sitter branch at a non-zero BEH radius. The new solutions have critical parameters $\tilde{\lambda}_{min}$ and $\tilde{\lambda}_{max}$ between which there are non-trivial solutions. $\tilde{\lambda}_{min}$ is determined by the ratio of the size of the structure to the size of the CEH, while $\tilde{\lambda}_{max}$ comes from the extremes of the solutions.

In order to specify whether the scalar hair we found is physical or not, we investigated the stability of new solutions by using a linear perturbation method. As a result all of the new solutions have negative eigenmodes and were found to be unstable. Thus the scalar hair is not real but a wig which falls off easily. Although we have considered only one real scalar field with a double well potential, we expect that the general no-scalar hair conjecture holds even if the cosmological constant exists.

Since these new solutions are unstable, the scalar field will be swallowed by the black hole and/or will escape to infinity over CEH. Then the solution becomes the stable Schwarzschild-de Sitter solution (a) with the same or smaller mass than the initial one. It is interesting to consider the development of the solution with maximum mass $\tilde{M} = 1/3$. Although a part of the scalar field escapes to infinity in the general case, it would be possible to set up the initial data where all the energy of the scalar field collapses into the black hole. If the third law of black hole thermodynamics is valid even in the present case, it should take an infinite amount of time for the black hole to swallow the scalar field and for the BEH to become degenerate with the CEH. It has been shown that similar phenomena occur in the evolution of the Kastro-Traschen solution [24], which can be interpreted as black holes with $Q = M$ are balanced to each other in CEH. For small black holes, they can coalesce to form a larger black hole. However when the size of the black holes is larger than a certain critical radius, coalescence does not occur even if we set the initial data to give the black holes a large initial velocity toward each other [25]. Our case would correspond to the critical case that the resultant BEH radius coincides with CEH.

As for the rotating case, the no-scalar hair conjecture can not been proved by using the techniques adopted in Ref. [4,10–12] even in the asymptotically flat case because they strongly depend on spacetime symmetry, i.e., staticity and spherical symmetry. On the other hand there is the beautiful result of the uniqueness theorem in the asymptotically flat case [2–6]. It seems worth investigating its counterpart in the asymptotic de Sitter case. At a first glance, however, we will soon find that the cosmological constant prevents us from constructing Ernst type equations and that different approaches are needed. We leave them open questions.

– Acknowledgments –

We would like to thank Dmitri V. Gal'tsov, Akio Hosoya, Hideki Ishihara and Kei- ichi Maeda for useful discussions and Julian McKenzie-Smith for his critical reading of our paper. This work was supported partially by the Grant-in-Aid for Scientific Research Fund of the Ministry of Education, Science and Culture (T.T. and K.M.), by the Grant-in-Aid for JSPS (No. 199704162(T.T.) and 199605200(K.M.)).

---

[1] R. Ruffini and J. A. Wheeler, Phys. Today B**24** 30 (1971).
[2] W. Israel, Phys. Rev. **164**, 1776 (1967); Commun. Math. Phys. **8**, 245 (1971); B. Carter, Phys. Rev. Lett. **26**, 331 (1971); R. M. Wald, Phys. Rev. Lett. **26**, 1653 (1971); D. C. Robinson, Phys. Rev. Lett. **34**, 905 (1977); P. O. Mazur, J. Phys. A **15**, 3173 (1982); Phys. Lett. A **100**, 341 (1984).
[3] J. E. Chase, Commun. Math. Phys. **19**, 276 (1970).
[4] J. D. Bekenstein, Phys. Rev. D**5**, 1239 (1972).
[5] J. B. Hartle, in *Magic without Magic*, edited by J. Klauder (Freeman, San Francisco, 1972).
[6] C. Teitelboim, Phys. Rev. D**5**, 2941 (1972).
[7] M. S. Volkov and D. V. Gal'tsov, Yad. Fiz. **51**, 1171 (1990) [Sov. J. nucl. Phys. **51**, 747 (1990)]; P. Bizon, Phys. Rev. Lett. **64**, 2844 (1990); H. P. Künzle and A. K. Masoud-ul-Alam, J. Math. Phys. **31**, 928 (1990).
[8] N. Straumann and Z.-H. Zhou, Phys. Lett. B **243**, 33 (1990); Z.-H. Zhou and N. Straumann, Nucl. Phys. **B360**, 180 (1991); P. Bizon, Phys. Lett. B **259**, 53 (1991); P. Bizon and R.M. Wald, Phys. Lett. B **267**, 173 (1991).
[9] M. S. Volkov, et al., Phys. Lett. B **349**, 438 (1995); O. Brodbeck, N. Straumann, J. Math. Phys. **37**, 1414 (1996).
[10] J. D. Bekenstein, Phys. Rev. D**51**, R6608 (1995).
[11] D. Sudarsky, Class. Quantum Grav. **12**, 579 (1995).
[12] M. Heusler, J. Math. Phys. **33**, 3497 (1992).
[13] M. Fukugita, F. Takahara, K. Yamashita and Y. Yoshii, Astrophys. J. **361**, L1 (1990).
[14] S. Perlmutter et al., Nature **391**, 51 (1998).
[15] T. Torii, K. Maeda and T. Tachizawa, Phys. Rev. D**51**, R6608 (1995).
[16] G. W. Gibbons and K. Maeda, Nucl. Phys. **B298**, 41 (1988); D. Garfinkle, G. T. Horowitz and A. Strominger, Phys. Rev. D **43**, 3140 (1991).
[17] S. J. Poletti, and D. L. Wiltshire, Phys. Rev. D **50** (1994) 7260; S. J. Poletti, J. Twamley, and D. L. Wiltshire, Phys. Rev. D **51** (1995) 5720.
[18] G. W. Gibbons and S. W. Hawking, Phys. Rev. D**15**, 2738(1977); S. W. Hawking and I. G. Moss, Phys. Lett. B **110**, 35 (1982).
[19] K. Nakao, gr-qc/9709014; K. Maeda, et al., Phys. Rev. D**57**, 3503 (1998).
[20] R. G. Cai and J. Y. Ji, SNUTP 97-120, gr-qc/9708064.
[21] T. Torii, K. Maeda and M. Narita, in preparation.
[22] R. Thom, *Strucure Stability and Morphogenesis*, Benjamin (1975); T. Poston and I. Stewart, *Catastrophe Theory and Its Applications*, Pitman, London (1978).
[23] K. Maeda, T. Tachizawa, T. Torii and T. Maki, Phys. Rev. Lett. **72**, 450 (1994); T. Torii, K. Maeda and T. Tachizawa, Phys. Rev. D. **51**,1510 (1995); T. Tachizawa, K. Maeda and T. Torii, Phys. Rev. D. **51**, 4054 (1995).
[24] D. Kastro and J. Traschen, Class. Quantum Grav. **13**, 2753 (1996).
[25] D. Brill, G. Horowits, D. Kastro and J. Traschen, Phys. Rev. D. **49**, 840 (1994).

Figure Captions

FIG. 1: The configurations of the scalar field $\tilde{\phi} = \sqrt{G}\phi$ with one node ($n = 1$). We set $\tilde{v} = \sqrt{G}v = 0.1$, $\tilde{\lambda} = \lambda/G\Lambda = 700$ and show the solutions for $\tilde{r}_B = \sqrt{\Lambda}r_B = 0.2$, 0.4, 0.6, 0.8. We also plot the regular solution without BEH by the dashed line for comparison. The left and right end points of each lines are BEH and CEH, respectively, and a dotted line traces them. As the BEH radius becomes large, the BEH coincides with the CEH and the solution becomes extremal.

FIG. 2: The configurations of the scalar field $\tilde{\phi} = \sqrt{G}\phi$ with one node ($n = 1$). We set $\tilde{v} = \sqrt{G}v = 0.1$, $\tilde{r}_B = \sqrt{\Lambda}r_B = 0.2$ and show the solutions for $\tilde{\lambda} = \lambda/G\Lambda = 400$, 700, 2000, 5000. As $\tilde{\lambda}$ becomes small, $\tilde{\phi}$ approaches zero and the solution coincides with the excited Schwarzschild-de Sitter solution (b) at $\tilde{\lambda} = \tilde{\lambda}_{min}$.

FIG. 3: The mass-BEH radius diagram of the new solutions. We set $\tilde{v} = \sqrt{G}v = 0.1$ and show the solutions for $\tilde{\lambda} = \lambda/G\Lambda = 300$, 400, 700, 2000, 5000. The dashed and dotted lines are the Schwarzschild-de Sitter solutions (a) and the excited Schwarzschild-de Sitter solutions (b), respectively. For small $\tilde{\lambda}$ there is a lower limit of the BEH, while we can take the BEH zero limit for the solution with large $\tilde{\lambda}$. The new solution branch and the exited Schwarzschild-de Sitter branch approach each other for large BEH and finally coincide. At this point the BEH and CEH degenerate and the solution becomes extremal.

FIG. 4: The critical parameters of the non-trivial solutions with $\tilde{r}_B = \sqrt{\Lambda}r_B = 0.6$ and $n = 1$. Between $\tilde{\lambda}_{max}$ and $\tilde{\lambda}_{min}$ curves there exist non-trivial solutions. We also plot the critical parameters of the regular solution by the dashed line for comparison. On the critical lines $\tilde{\lambda}_{mim}$ the non- trivial solutions coincide with the excited Schwarzschild-de Sitter solution (b). On the other hand the non-trivial solutions become extremal on the critical lines $\tilde{\lambda}_{max}$ with $\tilde{v} \gtrsim 0.14$, otherwise they correspond to the solution dotted in Fig. 3.

FIG. 5: (a) The configurations of the potential function $U$ of the linear perturbation equation for $\tilde{v} = \sqrt{G}v = 0.1$, $\tilde{\lambda} = \lambda/G\Lambda = 300$, $n = 1$ and $\tilde{r_B} = \sqrt{\Lambda}r_B = 0.4$, 0.6, 0.8. (b) The configurations of eigenmodes of the perturbation equation with the same parameters as (a). We find the only bound state ($m = 1$). The eigenvalue for each mode is $\tilde{\sigma}^2 = -0.4165$, $-0.1522$, $-0.0298$, respectively. (c) The eigenvalue of the linear perturbation equation for $\tilde{v} = \sqrt{G}v = 0.1$, $\tilde{\lambda} = \lambda/G\Lambda = 300$ and $n = 1$. Dotted lines are those of the excited Schwarzschild-de Sitter solution. At the point P where the non-trivial solution disappears, the excited mode of the Schwarzschild-de Sitter solution ($m = 1$) appears. This is consistent with the analysis made using catastrophe theory.

**Fig. 5(a)**

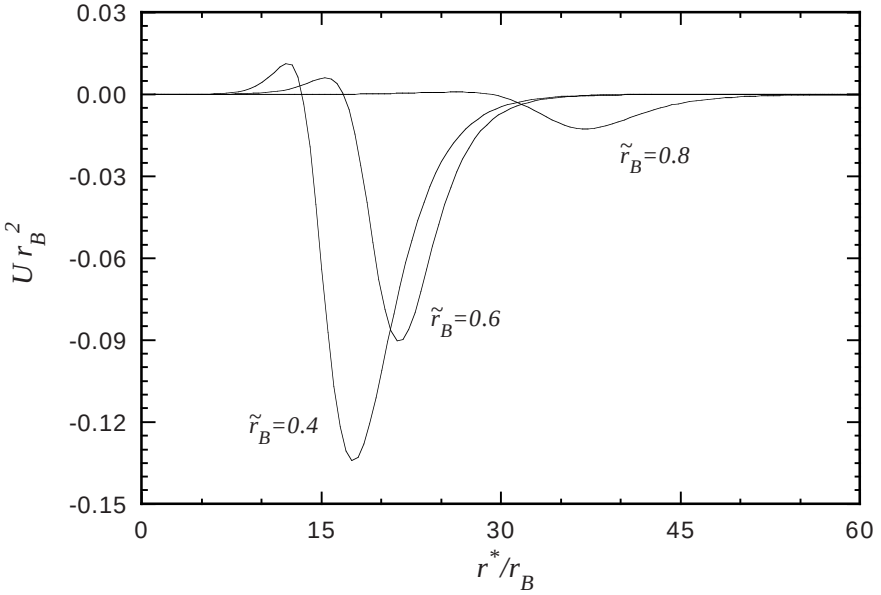


**Fig. 5(b)**

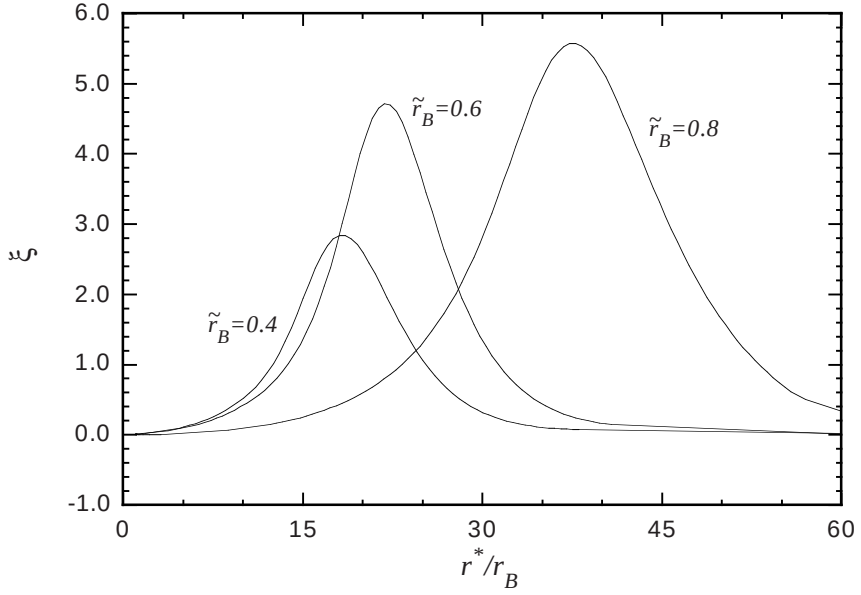


**Fig. 5(c)**

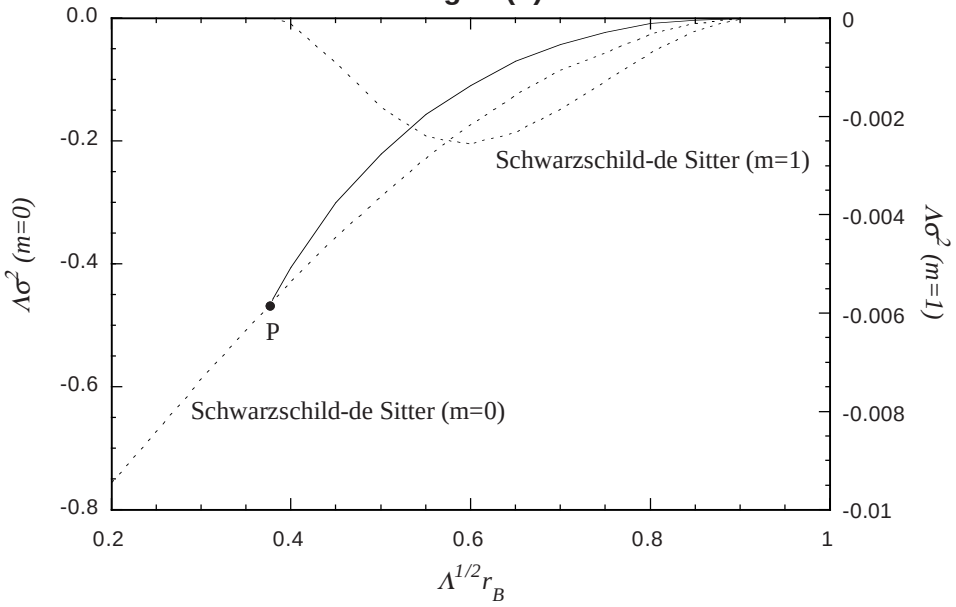

## Fig. 1

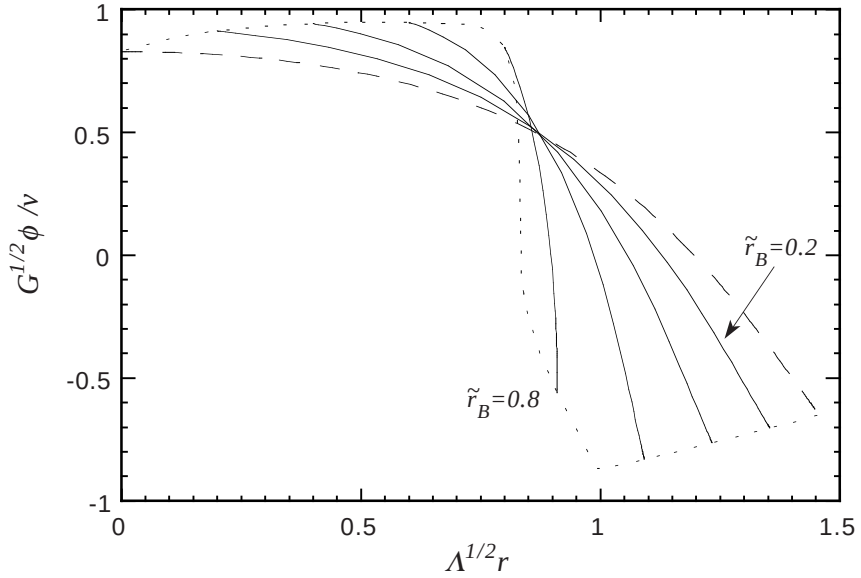


## Fig. 2

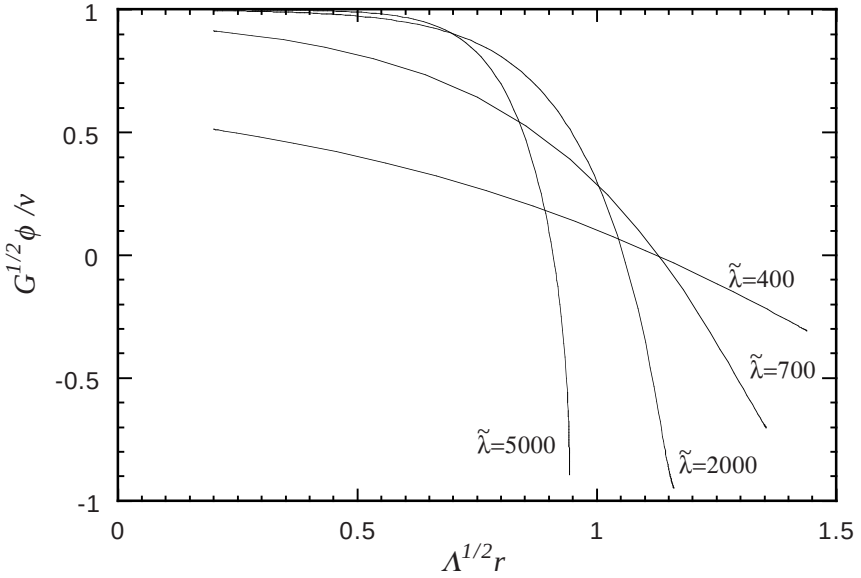


## Fig. 3

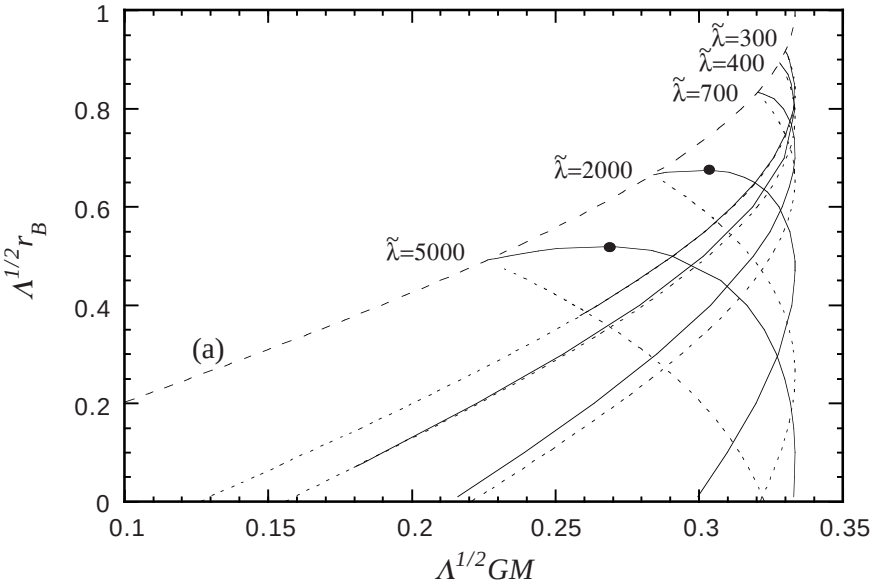


## Fig. 4